

# A low temperature cluster condensation approach to CdS nanocrystals: oxidative aggregation of $[\text{Cd}_{10}\text{S}_4\text{Br}_4(\text{Sp-Tol})_{12}]^{4-}$ with sulfur<sup>†</sup>

Frank E. Osterloh\* and Daniel P. Hewitt

Department of Chemistry, University of California at Davis, Davis, California 95616, USA.

E-mail: fosterloh@ucdavis.edu

Received (in West Lafayette, IN, USA) 27th February 2003, Accepted 23rd May 2003

First published as an Advance Article on the web 12th June 2003

The cluster salt  $[\text{N}(\text{C}_2\text{H}_5)_4][\text{Cd}_{10}\text{S}_4\text{Br}_4(\text{Sp-Tol})_{12}]$  reacts with six equivalents of sulfur in dimethylformamide at 140 °C to produce polycrystalline (wurtzite type) CdS nanoparticles of 5.8 nm mean diameter, which on their surface are ligated with *p*-tolylthiolate ligands, dimethylformamide and water; UV/vis, PL, <sup>1</sup>H- and <sup>113</sup>Cd-NMR spectra recorded during various stages of the synthesis indicate that the CdS nanoparticles are formed by a cluster condensation process.

The theoretical concept of using molecular clusters as synthetic precursors for the construction of crystalline inorganic solids is rooted in the recognition that certain transition element clusters contain structural fragments of the respective crystalline bulk phases.<sup>1–3</sup> The condensation of suitable clusters could offer a low energy pathway to crystalline solids, which otherwise are only accessible by high temperature solid state reactions. Despite the logic of this approach, examples for the successful application of this synthetic concept are extremely rare. Two examples are the reported condensation of  $[\text{Mo}_3\text{S}_{13}]^{2-}$  clusters to give crystalline  $\text{MoS}_2$  nanofibers<sup>4</sup> and the thermolysis of  $[\text{M}_{10}\text{Se}_4(\text{SPh})_{16}]^{4-}$  clusters (M = Cd, Zn) to produce CdSe and ZnSe nanocrystals.<sup>5</sup> In order to test the usefulness of the readily accessible  $[\text{Cd}_{10}\text{S}_4\text{Br}_4(\text{Sp-Tol})_{12}]^{4-}$  cluster anion<sup>6</sup> as a precursor to wurtzite phase CdS nanocrystals, we investigated its reactions with elemental sulfur in dimethylformamide/carbon disulfide. Because the tetra-adamantane core of the  $\text{Cd}_{10}$  cluster anion is a fragment of the cubic CdS (sphalerite) structure, oxidatively induced aggregation of this unit was expected to yield crystalline CdS nanoparticles under mild conditions.<sup>‡</sup>

When a solution of six equivalents of elemental sulfur in 0.5 mL carbon disulfide is added to a heated solution of 50 mg of the cluster salt  $(\text{Et}_4\text{N})_4[\text{Cd}_{10}\text{S}_4\text{Br}_4(\text{Sp-Tol})_{12}]$  (**1**, 140 °C) in 5 mL of DMF an immediate color change of the solution from pale to intense yellow indicates rapid aggregation of the cluster anion and formation of CdS nanocrystals. After 10 minutes, the reaction mixture is cooled to room temperature, and the nanocrystals are precipitated as a yellow-orange solid by addition of tetrahydrofuran. The nanocrystal yield is 87% based on Cd.

A transmission electron micrograph of the crude CdS nanocrystals is shown in Fig. 1 together with their size distribution, as determined by optical analysis of the micrographs. The particles have a mean diameter of 5.8 nm (std. 20%), and, due to the absence of organic surfactants, form weakly bonded aggregates that are readily soluble in polar solvents such as pyridine and DMF. The X-ray powder spectrum of the nanocrystals (ESI<sup>†</sup>) shows broad peaks typical of the hexagonal (wurtzite) form of CdS (JPS card 41-1049). Based on the half-width of the 110 reflection, the mean crystallite size of the particles is calculated as 3.5 nm using the Debye–Scherrer formula.<sup>7</sup> This value is smaller than the TEM diameter of 5.8 nm, but still within the error margins of both experiments. The UV/vis spectrum of the nanocrystals in DMF reveals an absorption edge of 430 nm, which corresponds to the

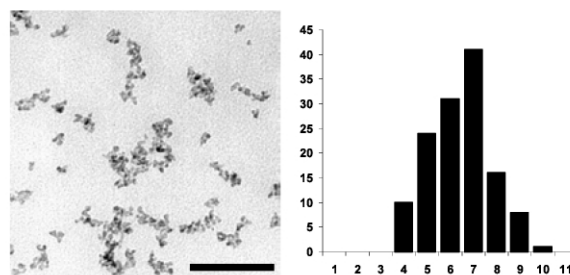


Fig. 1 Transmission electron micrograph of CdS nanocrystals formed by reaction of **1** with sulfur in hot DMF. Scale bar is 100 nm. A particle size histogram is also shown.

band gap excitation (2.88 eV). A comparison with the value for bulk CdS (2.42 eV)<sup>8</sup> shows that the CdS nanocrystals are in the size-confinement regime. The photoemission spectrum of the nanocrystals (inset of Fig. 2, curve C) looks remarkably similar to that of single nanocrystals<sup>9</sup> and has a maximum at unusually low energy, 492 nm. CdS nanocrystals of comparable size usually emit in the 440–460 nm range.<sup>10</sup> Both effects are likely consequences of the presence of residual  $\text{Cd}_{10}\text{S}_4$  fragments on the nanocrystal surface which provide trapping sites below the conduction band.

On the basis of their IR spectra (ESI), the as-synthesized CdS nanocrystals are ligated by a mixture of DMF, water, and *p*-tolylthiolate molecules. Bands around 2900–3000  $\text{cm}^{-1}$  are dominated by the C–H stretching vibrations of the DMF. The unsymmetrical O–H vibration of bound water (3600–3100  $\text{cm}^{-1}$ ) partially overlaps with this band. Evidence for the presence of coordinated thiocresol comes from three bands at 1082, 1013, 802  $\text{cm}^{-1}$ , which correspond to the ring vibration of 1,4-disubstituted benzene, and which can be observed at virtually the same positions in the free thiol. The C=O vibration

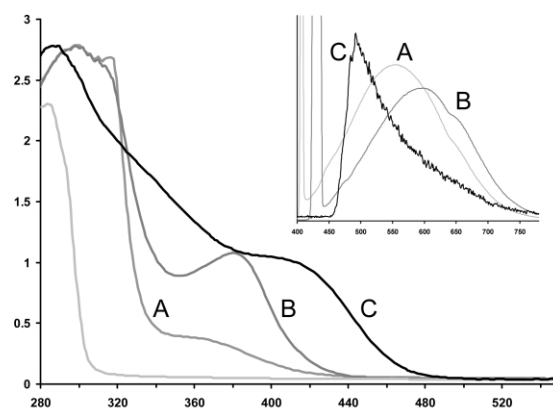


Fig. 2 UV/vis spectra (300 MHz,  $\text{DMF-d}_7$ ) of A) **1** before heating, B) **1** after 1 h at 100 °C, C) purified CdS nanocrystals in DMF. The spectrum of 4-methylphenylthiol (unmarked) is shown for comparison. Inset: emission spectra of **1** A) before heating ( $\lambda_{\text{ex}} = 400$  nm), B) after 1 h at 100 °C ( $\lambda_{\text{ex}} = 429$  nm), and C) purified CdS nanocrystals in DMF ( $\lambda_{\text{ex}} = 300$  nm).

<sup>†</sup> Electronic supplementary information (ESI) available: X-ray powder, IR and <sup>13</sup>C NMR spectra. See <http://www.rsc.org/suppdata/cc/b3/b302266h/>

of DMF appears as a strong band shifted to  $1636\text{ cm}^{-1}$  as is typical for coordinated DMF.

In order to elucidate the mechanism of nanocrystal formation, UV/vis, PL,  $^1\text{H}$  NMR and  $^{113}\text{Cd}$  NMR spectra were recorded during various stages of the nanocrystal synthesis. In DMF solution, the  $[\text{Cd}_{10}\text{S}_4\text{Br}_4(\text{SR})_{12}]^{4-}$  cluster anion gives rise to a broad absorption shoulder at  $364\text{ nm}$  (Fig. 2, spectrum A) and a luminescence with a maximum at  $557\text{ nm}$  (inset, spectrum A), in agreement with earlier measurements.<sup>6</sup> The  $^1\text{H}$  NMR spectrum (Fig. 3A) of the cluster salt contains doublets of *o*- and *m*-protons of cluster bound *p*-tolylthiolate ligands. However, additional weak pairs of doublets indicate that the cluster anion undergoes substitution of bromide by DMF to produce the species  $[\text{Cd}_{10}\text{S}_4\text{Br}_{4-x}(\text{DMF})_x(\text{SR})_{12}]^{(4-x)-}$  ( $x = 1\text{--}4$ ). Heating of the cluster solution to  $100\text{ }^\circ\text{C}$  under oxygen-free conditions for 5 min and then for 1 h (spectra B and C) completes the ligand substitution to produce the neutral cluster  $[\text{Cd}_{10}\text{S}_4(\text{DMF})_4(\text{SR})_{12}]$  (doublets at  $7.28$  and  $7.63\text{ ppm}$  for *m*- and *o*-protons of *p*-tolylthiolate ligands) traces of which can already be seen in spectrum A. Cases of intra- and intermolecular exchange of the terminal ligands have been documented for related Cd complexes and clusters.<sup>11,12</sup> The emission characteristics of the DMF ligated cluster ( $\lambda_{\text{max}} = 600\text{ nm}$ , B in inset of Fig. 2) are as expected very similar to **1**, whereas the absorption at  $364\text{ nm}$  (Fig. 2B) has grown in intensity and slightly shifted to  $382\text{ nm}$ .

The acquisition of  $^{113}\text{Cd}$  NMR data on **1** in DMF was problematic because of the low solubility of the salt in this solvent. In DMSO solution, however, **1** exhibits signals at  $567$  and  $651\text{ ppm}$  [vs. aqueous  $\text{Cd}(\text{ClO}_4)_2$ ], for the four outer and six inner  $\text{Cd}^{2+}$  sites respectively (ESI<sup>†</sup>). The  $651\text{ ppm}$  signal is broadened due to coupling with both inner and outer Cd ions.<sup>12</sup> After 1 h at  $100\text{ }^\circ\text{C}$ , the  $651\text{ ppm}$  (inner Cd sites) signal undergoes a shift to  $561\text{ ppm}$ , while the weaker signal at  $567\text{ ppm}$  (inner Cd

sites) can no longer be detected. This might be due to line broadening effects resulting from the coupling of  $^{113}\text{Cd}$  with the protons of DMSO.<sup>13</sup> When a solution of elemental sulfur is added to the hot solution of **1**, the absorption band at  $380\text{ nm}$  in the UV/vis spectrum immediately shifts to its final position at  $430\text{ nm}$  (spectrum C in Fig. 2), while the emission maximum of the solution in the PL spectrum moves to  $496\text{ nm}$  (spectrum C in inset). These spectral features are consistent with the formation of CdS nanocrystals. The  $^1\text{H}$  NMR spectrum in Fig. 3D reveals complete consumption of all cluster starting materials, and the formation of bis(4-toluy)disulfide as the major byproduct. The identity of the disulfide was confirmed by comparison with that of an authentic sample of the material obtained by oxidation of the thiol with iodine in hexane. The data suggest that CdS nanocrystal growth is driven by oxidative removal of the thiolate ligands on the  $\text{Cd}_{10}\text{S}_4$  cluster. This probably leads to unstable  $\text{Cd}_{10}\text{S}_{4+x}(\text{SR})_{12-2x}(\text{DMF})_4$  fragments ( $x = 1\text{--}6$ ) that subsequently condense into the CdS phase. These relatively soluble cluster fragments are likely to encapsulate the nanoparticle throughout the entire growth process and thus help to keep the nanoparticle in solution. This explains why no additional surfactants are needed in the synthesis. The efficiency of this cluster condensation process is not only illustrated by a  $5.8(1.2)\text{ nm}$  single domain size, which corresponds to  $930\text{--}3200$  condensed  $\text{Cd}_{10}$  clusters, but also by the low reaction temperature of  $140\text{ }^\circ\text{C}$ . This temperature is significantly below the temperature range routinely employed for the syntheses of CdS nanocrystals ( $250\text{--}300\text{ }^\circ\text{C}$ ) based on mononuclear (e.g. cadmium oxide and sulfur) starting materials,<sup>14–16</sup> indicating a different nanocrystal growth mechanism in our system. In conclusion we have demonstrated that crystalline CdS nanoparticles can be grown under mild conditions by reaction of cluster **1** with sulfur. This work confirms the value of molecular clusters as pre-assembled starting materials in the synthesis of inorganic nanocrystals.

## Notes and references

† The oxidative aggregation of the  $\text{Cd}_{10}\text{S}_4$  cluster with iodine has been previously investigated as an alternative pathway to CdS nanoparticles, but the products of this reaction were characterized only spectroscopically.<sup>17</sup>

- S. C. Lee and R. H. Holm, *Angew. Chem., Int. Ed. Engl.*, 1990, **29**, 840.
- D. Fenske, N. Y. Zhu and T. Langeteger, *Angew. Chem., Int. Ed.*, 1998, **37**, 2640.
- N. Y. Zhu and D. Fenske, *J. Chem. Soc., Dalton Trans.*, 1999, 1067.
- H. W. Liao, Y. F. Wang, S. Y. Zhang and Y. T. Qian, *Chem. Mater.*, 2001, **13**, 6.
- S. L. Cumberland, K. M. Hanif, A. Javier, G. A. Khitrov, G. F. Strouse, S. M. Woessner and C. S. Yun, *Chem. Mater.*, 2002, **14**, 1576.
- R. D. Adams, B. Zhang, C. J. Murphy and L. K. Yeung, *Chem. Commun.*, 1999, 383.
- H. P. Klug and L. E. Alexander, *X-Ray Diffraction Procedures for Polycrystalline and Amorphous Materials*, John Wiley & Sons, 1962.
- J. Cheon and J. I. Zink, *J. Am. Chem. Soc.*, 1997, **119**, 3838.
- S. A. Empedocles, R. Neuhauser, K. Shimizu and M. G. Bawendi, *Adv. Mater.*, 1999, **11**, 1243.
- W. W. Yu and X. Peng, *Angew. Chem., Int. Ed. Engl.*, 2002, **41**, 2368.
- P. W. Dean and J. V. Vittal, *Can. J. Chem.*, 1988, **66**, 2443.
- I. G. Dance, *Aust. J. Chem.*, 1985, **38**, 1745.
- L. Rodehuser, T. Chniber, P. Rubini and J. J. Delpuech, *Inorg. Chim. Acta*, 1988, **148**, 227.
- Z. A. Peng and X. G. Peng, *J. Am. Chem. Soc.*, 2001, **123**, 183.
- C. B. Murray, D. J. Norris and M. G. Bawendi, *J. Am. Chem. Soc.*, 1993, **115**, 8706.
- T. Vossmeier, L. Katsikas, M. Giersig, I. G. Popovic, K. Diesner, A. Chemseddine, A. Eychmuller and H. Weller, *J. Phys. Chem.*, 1994, **98**, 7665.
- T. Lover, G. A. Bowmaker, J. M. Seakins, R. P. Cooney and W. Henderson, *J. Mater. Chem.*, 1997, **7**, 647.

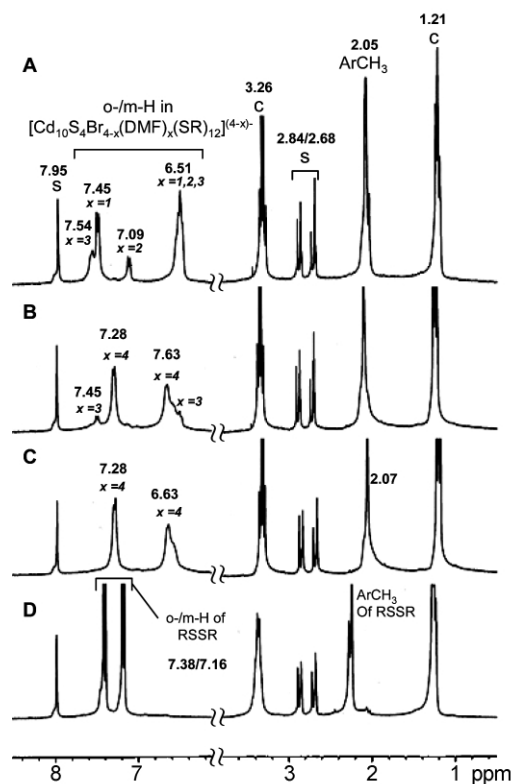


**Fig. 3**  $^1\text{H}$  NMR spectra (300 MHz,  $\text{DMF-d}_7$ ) of **1** A) before heating, B) after 5 min at  $100\text{ }^\circ\text{C}$ , C) after 1 h at  $100\text{ }^\circ\text{C}$ , D) after addition of sulfur. S and C denote solvent and tetraethylammonium cation. The free thiol gives doublets at  $7.16$  and  $7.04\text{ ppm}$ .